

## Interfacial Widths of Conjugated Polymer Bilayers

Cheng Wang,<sup>†</sup> Andres Garcia,<sup>‡</sup> Hongping Yan,<sup>†</sup> Karen E. Sohn,<sup>§</sup> Alexander Hexemer,<sup>||</sup>  
Thuc-Quyen Nguyen,<sup>‡</sup> Guillermo C. Bazan,<sup>\*,‡,§</sup> Edward J. Kramer,<sup>§,⊥</sup> and Harald Ade<sup>\*,†</sup>

Department of Physics, North Carolina State University, Raleigh, North Carolina 27695, Department of Chemistry and Biochemistry, University of California, Santa Barbara, California 93106, Advanced Light Source, Lawrence Berkeley National Laboratory, Berkeley, California 94720, Department of Materials, University of California, Santa Barbara, California 93106, and Department of Chemical Engineering, University of California, Santa Barbara, California 93106

Received June 26, 2009; E-mail: bazan@chem.ucsb.edu; harald\_ade@ncsu.edu

There is substantial challenge in being able to predict the bulk behavior of organic semiconductors on the basis of their molecular connectivity and composition.<sup>1</sup> Because of the weak intermolecular forces between structural units in comparison with inorganic counterparts, there is a strong dependence on processing history and therefore multiple morphologies, each with its own set of properties, can be obtained. Even more poorly understood are interfacial structures and their properties, either adjacent to metal electrodes or between different organic layers, despite their importance in regulating the overall performance of optoelectronic devices.<sup>2</sup>

It has been shown in polymer light-emitting diodes (PLEDs) that the introduction of a conjugated polyelectrolyte (CPE)<sup>3</sup> thin film between the electroluminescent layer and the cathode can be used to reduce the barrier to electron injection from environmentally stable cathodes such as Al or Au.<sup>4</sup> The interfaces in these devices have not been extensively studied yet are critical in mediating charge/exciton transport between layers.<sup>5</sup> Transmission electron microscopy (TEM) has been successfully used to characterize CPE/neutral conjugated polymer interfaces<sup>6</sup> and has shown that only materials cast from solvents of opposite polarity yield sharp interfaces and well-developed bilayer structures. However, quantitative measurements of the interfacial width [i.e., the root-mean-square (rms) width of the laterally averaged physical roughness and the chemical composition gradient normal to the interface] are difficult with TEM, and the interface could only be characterized as being  $\sim 2$  nm in width. Possible tools for high-precision characterization include neutron reflectivity<sup>7</sup> and X-ray reflectivity,<sup>8</sup> but these methods require deuteration of at least one component or suffer from low contrast,<sup>9,10</sup> respectively.

In this communication, we report high-precision measurements of organic/organic interfacial widths in CPE-containing model bilayers that are nearly isostructural to those successfully used for improving electron injection into PLEDs, as shown in Figure 1. We utilized resonant soft X-ray reflectivity (RSoXR), a method suitable for quantitative interface characterization that has high intrinsic material contrast for most polymer pairs.<sup>10,11</sup> In reflectivity, the partial reflections from the various interfaces interfere as a function of reflection angle. Since any roughness or chemical interdiffusion results in angle-dependent changes in the reflected intensity and hence the interference pattern, the width of the various interfaces can be inferred. PFN<sup>+</sup>X<sup>-</sup> [X<sup>-</sup> = Br<sup>-</sup>, tetrakis(imidazolyl)borate (BIm<sub>4</sub><sup>-</sup>)] was chosen as the CPE (see Figure 1 for chemical structures).<sup>12</sup> Bilayers were prepared by first casting an  $\sim 80$  nm thick poly[2-methoxy-5-(2'-ethylhexyloxy)-*p*-phenylene vinylene] (MEH-PPV) layer from toluene

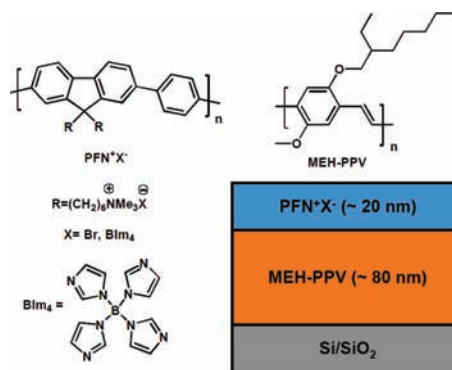


**Figure 1.** (left) Molecular structure of PFN<sup>+</sup>X<sup>-</sup>. (right) Nominal thin-film test structures.

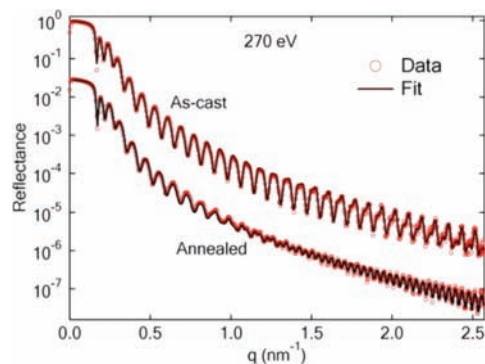


**Figure 2.** Reflectance of single as-cast and annealed MEH-PPV layers.

on oxide-covered silicon substrates. Casting of MEH-PPV was followed by spin-casting of an  $\sim 20$  nm thick PFN<sup>+</sup>X<sup>-</sup> layer from methanol. Some bilayers were created by casting atop a MEH-PPV layer that was previously thermally annealed at 240 °C. A bilayer structure was also heated to 240 °C for comparison. Finally, single MEH-PPV layers were also prepared to provide a reference for the initial surface roughness.

RSoXR data were acquired at beamline 6.3.2 at the Advanced Light Source (ALS) in Berkeley, CA,<sup>13</sup> following previously established protocols that avoid radiation damage.<sup>10</sup> Figure 2 presents plots of reflectance versus  $q$  obtained at 270 eV and their fits for the MEH-PPV reference layers. For the as-cast MEH-PPV surface, the fit yielded a Gaussian rms roughness of  $\sim 0.56$  nm (integrated over a sample area of  $\sim 80 \mu\text{m} \times 80 \mu\text{m}$ ); the surface is therefore very sharp and smooth. In contrast, fits for the thermally annealed MEH-PPV yielded an rms surface roughness of  $\sim 1.7$  nm, providing a rougher initial surface than the as-cast films. Examination of the MEH-PPV surface topography

<sup>†</sup> North Carolina State University.

<sup>‡</sup> Department of Chemistry and Biochemistry, University of California, Santa Barbara.

<sup>§</sup> Department of Materials, University of California, Santa Barbara.

<sup>||</sup> Lawrence Berkeley National Laboratory.

<sup>⊥</sup> Department of Chemical Engineering, University of California, Santa Barbara.

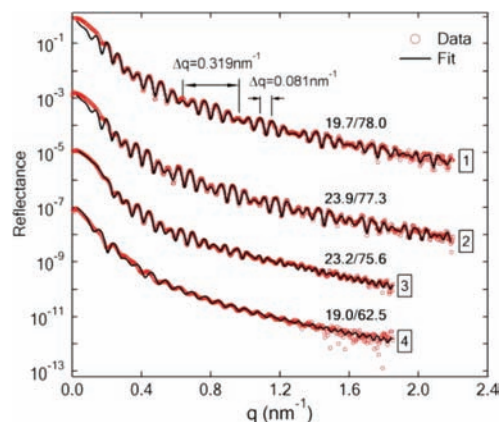


**Figure 3.** Reflectance data and fits for (1) PFN<sup>+</sup>Bim<sub>4</sub><sup>-</sup>/MEH-PPV, (2) PFN<sup>+</sup>Br<sup>-</sup>/MEH-PPV, (3) PFN<sup>+</sup>Br<sup>-</sup>/annealed MEH-PPV, and (4) annealed PFN<sup>+</sup>Br<sup>-</sup>/MEH-PPV bilayers, acquired at (1, 2) 285.4 and (3, 4) 285.6 eV. The larger  $\Delta q$  corresponds to the PFN<sup>+</sup>X<sup>-</sup> layer and its interfaces and the smaller  $\Delta q$  to the total polymer thin film. The pair of numbers next to each graph are the PFN<sup>+</sup>X<sup>-</sup> and MEH-PPV layer thicknesses (in nm) as measured with RSoXR.

**Table 1.** RSoXR Results from Fits

| Sample  | Surface Width (nm) | Average (nm) | Interfacial Width (nm) | Average (nm) |
|---|--------------------|--------------|------------------------|--------------|
| As-cast MEH-PPV   | Spot#1             | 0.53         | 0.56                   | N/A          |
|   | Spot#2             | 0.60         |                        |              |
| PFN <sup>+</sup> Br <sup>-</sup> /MEH-PPV               | Spot#1             | 0.67         | 0.85                   | 0.80         |
|   | Spot#2             | 0.63         | 0.74                   |              |
| PFN <sup>+</sup> Bim <sub>4</sub> <sup>-</sup> /MEH-PPV | Spot#1             | 0.74         | 0.85                   | 0.82         |
|   | Spot#2             | 0.69         | 0.79                   |              |
| Annealed MEH-PPV  | Spot#1             | 1.7          | 1.7                    | N/A          |
|   | Spot#2             | 1.7          |                        |              |
| PFN <sup>+</sup> Br <sup>-</sup> /Ann.. MEH-PPV         |                    | 1.6          |                        | 2.0          |
| Annealed PFN <sup>+</sup> Br <sup>-</sup> /MEH-PPV      |                    | 1.1          |                        | 4.0          |

by atomic force microscopy (AFM) provided rms results that are consistent with those obtained by RSoXR (see the Supporting Information).

RSoXR plots of the two CPE/MEH-PPV bilayers on as-cast MEH-PPV are presented in Figure 3, along with data for a bilayer of PFN<sup>+</sup>Br<sup>-</sup> cast atop annealed MEH-PPV. Modulations of the Kiessig fringes reminiscent of interference beats are readily observable for all of the bilayers. These modulations are distinct from the fringes observable in Figure 2 and directly indicate sensitivity to the buried organic/organic interface. Qualitative differences depending on whether the MEH-PPV was thermally annealed can also be readily observed. Because of the larger roughness of the interface in the former sample, the beating is suppressed. Through fits as shown in Figure 3, quantitative values for the widths of the surface and the CPE/polymer interface were extracted, and the results are summarized in Table 1. As-cast bilayers have smooth interfaces with average rms widths of 0.80 and 0.82 nm for PFN<sup>+</sup>Br<sup>-</sup>/MEH-PPV and PFN<sup>+</sup>Bim<sub>4</sub><sup>-</sup>/MEH-PPV, respectively. The CPE/MEH-PPV interfacial widths are only slightly larger than the surface roughness of the MEH-PPV reference layer.

As evidenced even in the raw data in Figures 2 and 3, the surface and interfacial widths can be greatly affected by the sample preparation procedure. The interfacial roughness for the PFN<sup>+</sup>Br<sup>-</sup>/annealed MEH-PPV bilayer is 2.0 nm, an increase of 0.3 nm relative to the preannealed MEH-PPV surface. This clearly demonstrates that casting does not smooth out the interface. The PFN<sup>+</sup>Br<sup>-</sup>/MEH-PPV bilayer that was

thermally annealed (included only for illustrating RSoXR) shows a markedly different reflectance profile because of an interfacial width of 5.9 nm.

The increased widths observed for the as-cast bilayers relative to that of the starting MEH-PPV surface could be due to roughening (lack of smoothness) or chemical interdiffusion (lack of sharpness). However, AFM (see the Supporting Information) shows dominating lateral structures >10 nm in size for the initial MEH-PPV surface. This is significantly larger than the measured interfacial width. Consequently, in conjunction with the observation that casting on rough MEH-PPV does not result in smoother interfaces, it is highly likely that the physical roughness of the interface does not decrease for the as-cast films. Since these as-cast samples with a very thin top layer do not have frozen-in capillary waves,<sup>14</sup> the chemical interdiffusion and physical roughness add quadrature to the rms width; the upper limit for the chemical interdiffusion is thus  $(0.81^2 + 0.56^2)^{1/2} = 0.59$  nm.

In conclusion, we have shown that the interfaces of differentially cast CPE/MEH-PPV bilayers can be very smooth and sharp. This demonstrates with high precision that the MEH-PPV layer is not much disturbed by casting the CPE layer from a polar solvent. The chemical interdiffusion due to casting is limited to less than 0.6 nm, as the increase in width observed might be partially due to roughening. The interface created is thus nearly “molecularly” sharp. These results establish a baseline for understanding the role of interfacial structure in determining the performance of CPE-based PLEDs. More broadly, we anticipate further applications of RSoXR in achieving a deeper understanding of other multilayer organic optoelectronic devices, including multilayer photovoltaic devices.

**Acknowledgment.** The authors acknowledge support by the Department of Energy (DE-FG02-98ER45737) and the National Science Foundation (UCSB MRL, DMR 0520415, DMR 0606414, CAREER DMR 0547639, and NSF Graduate Fellowship). Data were acquired at beamline 6.3.2 at the ALS (supported by DOE Contract DE-AC02-05CH11231).

**Supporting Information Available:** Synthetic and device-fabrication procedures, RSoXR data acquisition and analysis, and AFM images. This material is available free of charge via the Internet at <http://pubs.acs.org>.

## References

- (1) Bazan, G. C. *J. Org. Chem.* **2007**, *72*, 8615.
- (2) (a) Cahen, D.; Kahn, A. *Adv. Mater.* **2003**, *15*, 271. (b) Higgins, A. M.; Cadby, A.; Lidzey, D. C.; Dalgliesh, R. M.; Geoghegan, M.; Jones, R. A. L.; Martin, S. J.; Heriot, S. Y. *Adv. Funct. Mater.* **2009**, *19*, 157.
- (3) Jiang, H.; Taranekekar, P.; Reynolds, J. R.; Schanze, K. S. *Angew. Chem., Int. Ed.* **2009**, *48*, 4300.
- (4) Hoven, C. V.; Yang, R. Q.; Garcia, A.; Crockett, V.; Heeger, A. J.; Bazan, G. C.; Nguyen, T. Q. *Proc. Natl. Acad. Sci. U.S.A.* **2008**, *105*, 12730.
- (5) Hoven, C. V.; Garcia, A.; Bazan, G. C.; Nguyen, T. Q. *Adv. Mater.* **2008**, *20*, 3793.
- (6) Steuerman, D. W.; Garcia, A.; Dante, M.; Yang, R.; Lofvander, J. P.; Nguyen, T. Q. *Adv. Mater.* **2008**, *20*, 528.
- (7) (a) Jones, R. A. L. *Polymers at Surfaces and Interfaces*; Cambridge University Press: New York, 1999. (b) Higgins, A. M.; Martin, S. J.; Geoghegan, M.; Heriot, S. Y.; Thompson, R. L.; Cubitt, R.; Dalgliesh, R. M.; Grizzi, I.; Jones, R. A. L. *Macromolecules.* **2006**, *39*, 6699.
- (8) (a) Lee, Y. J.; Lee, H.; Byun, Y.; Song, S.; Kim, J. E.; Eom, D.; Cha, W.; Park, S. S.; Kim, J.; Kim, H. *Thin Solid Films* **2007**, *515*, 5674. (b) Lee, Y. J.; Li, X.; Kang, D. Y.; Park, S. S.; Kim, J.; Choi, J. W.; Kim, H. *Ultramicroscopy* **2008**, *108*, 1315.
- (9) (a) Seeck, O. H.; Kaendler, I. D.; Tolan, M.; Shin, M.; Rafailovich, M. H.; Sokolov, J.; Kolb, R. *Appl. Phys. Lett.* **2000**, *76*, 2713. (b) Ade, H.; Wang, C.; Hexemer, A.; Garcia, A.; Nguyen, T.-Q.; Bazan, G. C.; Sohn, K. E.; Kramer, E. J. *J. Polym. Sci., Part B: Polym. Phys.* **2009**, *47*, 1291.
- (10) Wang, C.; Araki, T.; Watts, B.; Harton, S.; Koga, T.; Basu, S.; Ade, H. *J. Vac. Sci. Technol., A* **2007**, *25*, 575.
- (11) Wang, C.; Araki, T.; Ade, H. *Appl. Phys. Lett.* **2005**, *87*, 214109.
- (12) Yang, R.; Wu, H.; Cao, Y.; Bazan, G. C. *J. Am. Chem. Soc.* **2006**, *128*, 14422.
- (13) Underwood, J. H.; Gullikson, E. M. *J. Electron Spectrosc.* **1998**, *92*, 265.
- (14) Sferazza, M.; Xiao, C.; Jones, R. A. L.; Bucknall, D. G.; Webster, J.; Penfold, J. *Phys. Rev. Lett.* **1997**, *78*, 3693.

JA905293M